



A novel co-contaminated sediment treatment approach: *Quercus petraea* leaf-extracted nZVI supported on native clay and biochar for potentially toxic elements and PAHs removal

Nataša Slijepčević¹ · Dunja Rađenović¹ · Jelena Beljin¹ · Gábor Kozma² · Zoltán Kónya² · Snežana Maletić¹ · Dragana Tomašević Pilipović¹

Received: 30 January 2023 / Accepted: 30 October 2023 / Published online: 17 November 2023
© The Author(s), under exclusive licence to Springer-Verlag GmbH Germany, part of Springer Nature 2023

Abstract

Purpose Sediment contamination is complex, and it is challenging to find the solution that corresponds to treating different groups of pollutants effectively. The existence of potentially toxic elements and polycyclic aromatic hydrocarbons in co-contaminated river sediment contributes serious toxic residues to the environment. Thus, it is crucial to involve remediation techniques that simultaneously remove these two complex groups of pollutants. Also, a significant challenge is due to the complex interactions between these groups of contaminants and the sediment matrix.

Methods Iron-based materials, such as green produced nano-zero-valent iron, are advantageous, environmentally friendly, and interest in their use is growing. This study demonstrates the potential of green nZVI supported by native clay and biochar for the simultaneous removal of potentially toxic elements and PAHs from co-contaminated river sediment.

Results It was indicated that potentially toxic elements removal was better than the removal of PAHs, but the removal of both groups of contaminants was noticeable with no further impact to the environment. The results showed which mechanisms played key roles in removal of pollutants from the river sediment. Additionally, extraction tests showed that sediment treated with modified iron nanoparticles is non-hazardous and that it represented promising results in removal of organic and inorganic pollutants.

Conclusion Green synthesis of nZVI by oak leaf extract (*Quercus petraea*) and supported materials (native clay and biochar) was valuable for recycling wastes and creating treated sediment for potential further beneficial sustainable use.

Keywords Sediment · Metals · PAHs · Green synthesized nZVI · Synergistic removal

1 Introduction

Sediment in rivers near industrial plants or large cities that do not have adequate wastewater treatment usually contains polycyclic aromatic hydrocarbons

(PAHs) and potentially toxic elements together, among other compounds. Contamination by these hazardous contaminants draws attention globally, because of their cytotoxic effects (Staninska-Pieta et al. 2020). The removal of these contaminants and the remediation of the sediment represent a decades-long challenge in terms of finding a treatment that is efficient,

Responsible editor: Sophie Ayrault

✉ Dunja Rađenović
dunja.radjenovic@dh.uns.ac.rs

Nataša Slijepčević
natasa.slijepcevic@dh.uns.ac.rs

Jelena Beljin
jelena.spasojevic@dh.uns.ac.rs

Gábor Kozma
kozmag@chem.u-szeged.hu

Zoltán Kónya
konya@chem.u-szeged.hu

Snežana Maletić
snezana.maletic@dh.uns.ac.rs

Dragana Tomašević Pilipović
dragana.tomasevic@dh.uns.ac.rs

¹ Department of Chemistry, Biochemistry and Environmental Protection, Faculty of Sciences, University of Novi Sad, Trg Dositeja Obradovica 3, 21000 Novi Sad, Serbia

² Interdisciplinary Excellence Centre, Department of Applied and Environmental Chemistry, University of Szeged, Rerrich Béla Tér 1, Szeged 6720, Hungary

economically acceptable and causes the least damage to the environment (Zhang et al. 2021; Maletic et al. 2022). The application of nanotechnologies, especially materials synthesized by “green” methods, in environmental remediation processes has been constantly increasing over the years due to low treatment costs and constant improvement of the quality of applied remediation processes. Nano zero-valent iron (nZVI) is considered as promising material for the elimination of contaminants from the environment including potentially toxic elements and/or organic compounds, as well as nitrates (Wang et al. 2017; Li et al. 2019; Guo et al. 2022). It has been established that nZVI can be synthesized in methods which require specific expensive costs, huge amounts of energy, and toxic chemicals like NaBH_4 . Therefore, eco-friendly and non-hazardous, bio-based “green” synthesized methods for nZVI have been developed and used in this research. Previous studies have reported that green synthesized nZVI from plant extracts has been used for the removal of metals (Poguberović et al. 2016; Stefaniuk et al. 2016; Francy et al. 2020; Slijepčević et al. 2021). However, nZVI alone has the tendency to aggregate so researchers developed new stabilized nZVI material using zeolite (Li et al. 2020), kaolinite (Lakkaboyana et al. 2021), activated carbon (Li et al. 2022), and bentonite (Diao and Chu 2021). Clays have large specific surface area and high cation exchange capacity (CEC), which make it suitable for hosting nZVI and binding anions or cations of the pollutants through ion exchange or adsorption. Ions can also be adsorbed at the edges of the clay crystal lattice and exchange with other ions in the water/sediment (Patel et al. 2008). In the few last years, researchers have been using biochar (BC) as a supporter of nZVI for improving his dispersibility, due to BC porous structure, high adsorption capacity, and high specific surface area (Wang et al. 2017; Li et al. 2022, 2023). Some studies showed that BC on nZVI effectively enhances the removal efficiencies of pollutants (Liu et al. 2021; Ahmad et al. 2022). As has been stated before, co-contamination with potentially toxic elements and PAHs represents a major concern for the environment, and therefore, it is crucial to understand the mechanisms and influences associated with the use of green-synthesized nZVI from oak leaf extract (OL-nZVI) supported on biochar and clay in sediment. While some literature exists regarding such application in terms of one or two selected contaminants, a systematic view on this real situation where different mechanisms are included, and different compounds are competing for active place on nanomaterial, is lacking.

In this study, six potentially toxic elements and 16 EPA PAHs were selected as the targets. The aim of this study was to compare, determine, and investigate the effect of

OL-nZVI (green nZVI) supported on biochar and native clay on the total and bioavailable content of metals and PAHs in river sediment. Additionally, the main objectives of this study were to (1) synthesize and characterize nZVI from oak leaf extract supported on biochar and clay; (2) examine of the current status of PAHs and potentially toxic elements concentration in river sediment; (3) investigate the efficiency of immobilization sediment treatment through sequential extraction, leaching tests on metals, and single step XAD-4 extraction on PAHs; and (4) explore the possible reaction mechanism for immobilization of potentially toxic elements and PAHs.

2 Materials and methods

2.1 Sediment sampling

Sediment samples were taken from Danube-Tisa-Danube (DTD) river system, i.e., Great Bačka Canal according to the standard method SRPS ISO 5667–12 (SRPS ISO 5667–12:2019). The Great Bačka Canal is part of the DTD drainage network, which connects the Danube and Tisa river flows in Northern Serbia (Vojvodina) at the Pannonian Basin’s southern margin. The canal is 118 km long and connects the Danube at Beždan to the Tisa at Becej. The canal became polluted in the second half of the twentieth century as a result of rapid industrial development and inadequate wastewater treatment, with effluents discharged directly into the recipient. The Eijkelkamp “core sampler” was used to collect undisturbed sediment by depth (water depth ranging from 2.0 to 5.5 m) in the middle of canal. Surface sediment profile was investigated for chemical characterization of the sediment. The criteria for selecting sampling points was based on previous studies of the spatial distribution of industries and related pollution (Krčmar et al. 2017). The samples were collected in glass jars (for analysis of PAHs) and plastic containers (for analysis of potentially toxic elements), kept in fridge on 4 °C, and also stored after delivery to the laboratory until they were ready for analysis. To minimize sample contamination, all materials were used for sampling, treatment, and storage of samples, and solutions were carefully selected, acid-cleaned, and conditioned (EPA 2004). The sediment samples were air dried and homogenized in accordance with ISO 11464:2006 method, and then they were passed through a 250 μm sieve (ISO 565:1990) and characterized for the following parameters: determination of pH value was measured according to method SRPS ISO 10390:2007, organic matter (also moisture) by method (SRPS EN 12879:2007), and clay content, fraction < 2 mm, was determined according to the standard method (ISO 11277:2009). Metals extraction from sediment sample was performed according to microwave digestion (milestone

start E) by method of EPA 3051a (USEPA 2007a), and also sequential extraction was performed for metal distribution in sediment sample by Jamali et al. (2009) (RSD < 5%, $n = 3$). Concentration of PAHs in sediment was determined with following steps: after extraction using ultrasound (EPA Method 3550B, USEPA 1995) and purification on silica gel (EPA Method 3630C, USEPA 1996a) then GC/MS analysis (EPA Method 8270D, USEPA 1996b) was performed. Results for PAH content and potentially toxic elements were calculated on dry sediment mass. The results of metals and PAHs concentrations are considered in reference to Serbian regulation (“Off. Gazette of RS,” No. 50/2012). Mean values was used and the RSDs ($n = 3$) have been below 5%.

2.2 Preparation of nanomaterials

Synthesis procedure of OL-nZVI is described and taken from Slijepcevic et al. (2021). In order to improve performance of this nanomaterial, some modifications were included in the procedure, addition of native clay and biochar as good adsorbents of pollutants. Preparation of NC-gnZVI implied dissolving native clay in 0.1 M $\text{FeCl}_3 \cdot 6\text{H}_2\text{O}$ and stirring for 120 min (Soliemanzadeh and Fekri 2017) using a magnetic stirrer to form a homogenous suspension. The composition of the native clay which was used from the area of Vojvodina (locality of Potisje, Kanjiža, Serbia) was as followed (wt.%): SiO_2 (55.7), Al_2O_3 (14.91), Fe_2O_3 (5.78), MgO (2.86), CaO (5.9), Na_2O (0.83), K_2O (0.14), SO_3 (0.22), TiO_2 (0.8), and loss on ignition has been 10.58% (Kerkez et al. 2014). Biochar (BC) used in this study is commercially available from wholesale and has European Biochar Certificate (EBC 2012–2022). KonTiki system using hard wood with charring temperature around 680 to 740 °C has made this biochar. Preparation of BC-gnZVI has started with dissolving biochar in 0.1 M $\text{FeCl}_3 \cdot 6\text{H}_2\text{O}$, and stirring for 30 min, using a magnetic stirrer. The mass ratio of biochar to Fe has been 1:2 (Zhang et al. 2020). During stirring time in both cases, oak leaves extract was prepared by Machado et al. (2013). Subsequently, the filtered oak extract was added by drop wise to 0.1 M of $\text{FeCl}_3 \cdot 6\text{H}_2\text{O}$ (native clay mixture) and also 0.1 M of $\text{FeCl}_3 \cdot 6\text{H}_2\text{O}$ (biochar mixture at a volume ratio of 3:1 at room temperature with continuous stirring). The black particles that appeared were centrifuged and washed three times with ethanol. Furthermore, wet paste was dried and used in the experiment.

2.3 Characterization of nanomaterial

The OL-nZVI, NC-gnZVI, and BC-gnZVI were characterized by using BET, TEM, SEM/EDS, XRD, and FTIR techniques. The following Brunauer, Emmett, and Teller method (BET), was used to determine the specific surface area using the Autosorb iQ Surface Area Analyzer (Quantachrome Instruments, USA). Images of transmission

electron microscopy (TEM; Philips CM 10) and scanning electron microscopy (SEM/EDS; Hitachi S171 4700 TypeII) were reported to define morphology, size, and particle distribution of the three different nanomaterials. X-ray diffraction (Philips PW1710 automated X-ray powder diffractometer, USA) was used to identify the mineral composition, i.e., metal oxides and metal hydroxides. Thermo-Nicolet Nexus 670 apparatus was used for FTIR analysis.

2.4 Treatment of sediment

The optimal mass percentage of green nanomaterials which was added to the sediment, and which has showed the most effective results is 5%, as was described by the research paper Slijepčević et al. (2018, 2021). Therefore, the mentioned mass percentages were also observed in this work. The mixtures of sediment with 5% by weight OL-nZVI, NC-gnZVI, and BC-gnZVI were further prepared according to ASTM D1557-00 procedure. This test method covers laboratory method which was used to determine compaction characteristics of soil/sediment using modified effort (56,000 ft-lbf/ft³ (2,700 kN-m/m³)). The mixtures after compaction were placed in inert plastic bags and left to stand for 28 days at a temperature of 20 °C. After that, the mixtures were cut to obtain cubes with dimensions of $3 \pm 0.3 \text{ cm} \times 3 \pm 0.3 \text{ cm} \times 3 \pm 0.3 \text{ cm}$. Then samples (cubes) were smashed and applied for various leaching tests for concentration of metals and a single step XAD-4 extraction, as method for bioavailability assessment of PAH, to determine the character of the final material. Leaching tests which were used in this experiment are Toxicity Characteristic Leaching Procedure (TCLP) (USEPA 2002) and German standard test—DIN 3841-4 S4 (1984); two single extraction methods have been performed to assess the metal bioavailability: extraction with diluted EDTA (Quevauviller et al. 1997) and HCl (Sutherland 2002). Microwave-assisted extraction procedure (MWSE) was also done for treated sediment samples as it was described by Jamali et al. (2009). A fast microwave-assisted extraction procedure was developed and proposed by modified BCR protocol (the community Bureau of Reference now the European Union “Measurement and Testing Programme”). Optimization of MW power and extraction time was performed under carefully controlled conditions of extraction solution temperature, which has not been higher than 50 °C, and the solutions were never brought to boiling. The fine powdered sediment samples of 0.2500 g were mineralized using a microwave-assisted acid digestion system. The extraction includes four steps of samples digestion (the first with addition of 0.11 M acetic acid solution, the second with 0.5 M hydroxylamine hydrochloride solution, the third with 5% H_2O_2 and 1 M ammonium acetate, and the fourth includes addition of aqua regia (HCl/HNO₃, 3:1)). The microwave-based digestion conditions

have included microwave induced time from 90 to 120 s, 800 psi pressure, and 1200 W power. Metals concentrations were analyzed on an atomic absorption spectrometer (Perkin Elmer AAnalyst™ 700) according to the procedure EPA 7010 (USEPA 2007c) and 7000b (USEPA 2007b). In the determination of desorption through XAD-4 extraction, we employed the method outlined by Cornelissen et al. (1997) with modifications as previously described in studies by Spasojevic et al. (2015, 2018) and Roncevic et al. (2016).

3 Results and discussion

3.1 Characterization of nanomaterials (OL-nZVI, NC-gnZVI and BC-gnZVI)

Characterization of nano zero-valent iron synthesized from oak leaves extract has already been described in detail from previous research by Slijepčević et al. (2021), where results demonstrated that OL-nZVI is nontoxic and it is stable nanomaterial for application in the sediment remediation. The use of supporting agents like native clay and biochar in nanoparticle synthesis enhance dispersion reduces potential agglomeration and also improves adsorption capacity of nanoparticles. These two porous materials were chosen based on their many characteristics, as well as the efficiency that clays and biochar showed in the case of stabilizing iron nanoparticles and their further application in the treatment of contaminated environment matrixes (Slijepčević et al. 2018, 2021; Oleszczuk and Koltowski 2017; Solimanzadeh and Fekri 2017; Tomašević Pilipović et al. 2018; Ruiz-Torres et al. 2018; Qiao et al. 2018; Wang et al. 2019a). Using BET structural analysis, a lower value of the specific surface area of stabilized nanoparticles was observed than that of the native clay itself (Table S1). The lower value of the specific surface is due to the fact that the surface of the green nanoparticles is covered with organic molecules that are an integral part of polyphenols and other macromolecules found in the extract of oak leaves (Slijepčević et al. 2021). The decreased specific surface area was also noticed in the case of biochar, and this may be because the pore structure of biochar was blocked by dispersed nanoparticles. Similar aspect that biochar pore structure can affect the oxidation and crystallite size of nanoparticles was described in a review paper by Wang et al. (2019a).

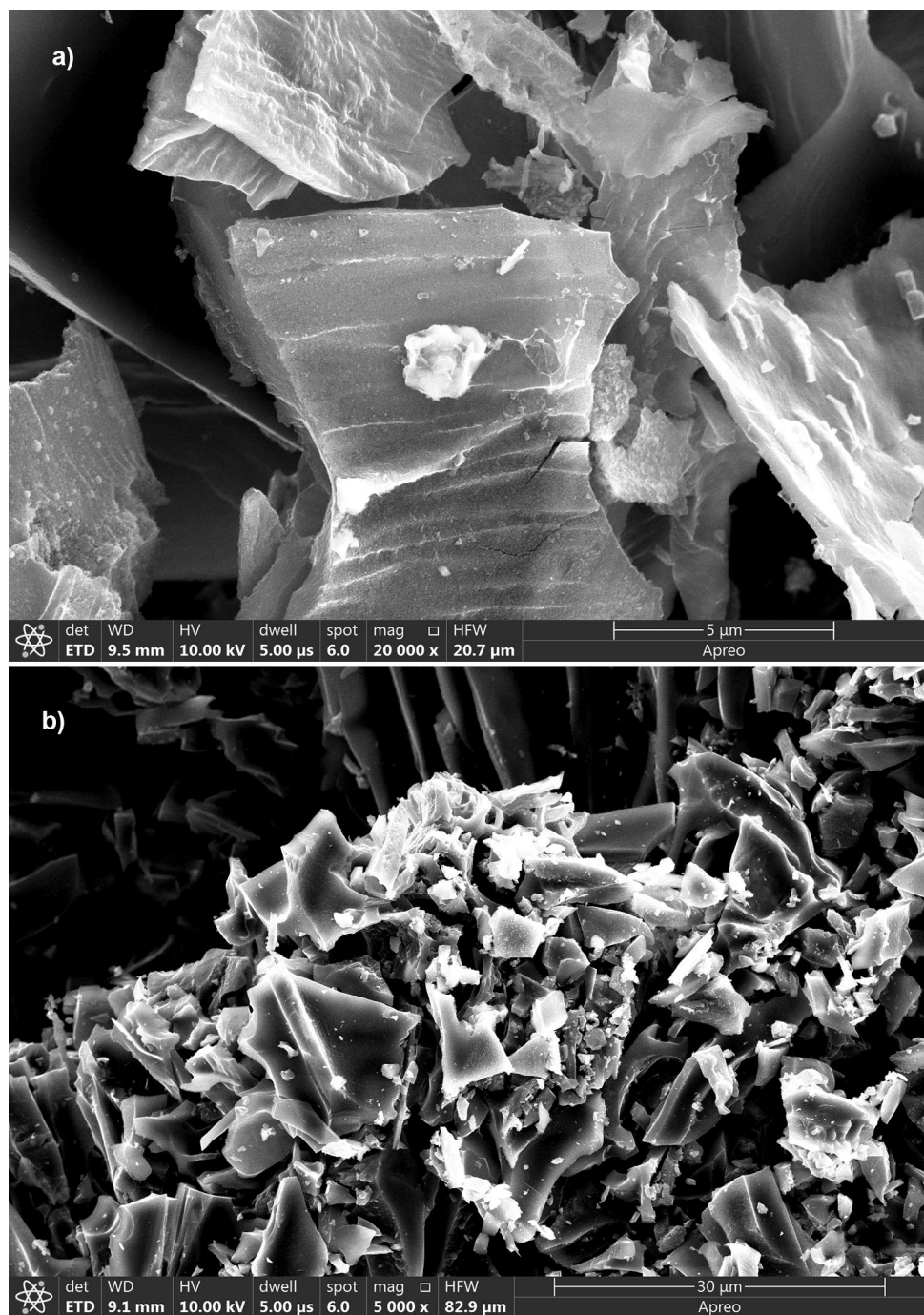
The results showed (Fig. 1b) that nZVI in the range of 40–60 nm were located on the surfaces of native clay, generally spherical in shape. When we look at the SEM micrograph of native clay (Fig. 1a) with smooth and glossy layers with a few gorges, it is logical that it represents a good supporting material for nano zero-valent iron. EDS analysis (Table S2) indicates the presence of O, Si, Al, and Mg, in the both samples. TEM image of the NC-gnZVI (Fig. S1) showed that Fe nanoparticle successfully supported on the

native clay surface. Similar results have been reported in previous studies (Solimanzadeh and Fekri (2017) and Husen and Iqbal (2019)).

Biochar (Fig. 2a) was characterized by porous and smooth surface structure (Zhang et al. 2019). After synthesis of BC-gnZVI, formed nanoparticles were randomly located, evenly dispersed and roughened the biochar surface. These nanoparticles were spherical, discrete, and dispersed with a mean diameter of about 100 nm. The EDS data in Table S2 shows that the principal compositions in the biochar were C 56.32 wt%; O 39.5 wt%; Mg 1.61 wt%, and Na 0.72 wt%. The Fe content in BC-nZVI was 21 times higher than in biochar alone, indicating that iron was successfully impregnated in BC. The high concentration of Cl in both nanomaterials is attributed to the FeCl₃ salt, which was used for the synthesis of nanoparticles. The elements potassium and calcium also present in NC-gnZVI and BC-gnZVI come from the plant extract. They are essential for plant growth and exist in every living plant cell (Kecic et al. 2018). Based on TEM image (Fig. S2), the nanoparticles were spherical and imbedded in biochar matrix, where the carbon support effectively inhibits agglomeration (Zhang et al. 2019). The X-ray patterns of NC-gnZVI and BC-gnZVI presented in Fig. 3 showed the presence of the main diffraction peak at a 2θ value of 44.9° which is associated with the load of nZVI to the native clay layers/biochar, respectively.

The XRD diffractogram (Fig. 3a) also identified peaks corresponding to the structure of kaolinite, montmorillonite, and smaller peaks originating from the internal structure of clay (Shi et al. 2011; Solimanzadeh and Fekri 2017; Slijepčević et al. 2021), and also a large diffraction peak at 29.5° in XRD pattern of biochar (Fig. 3b) corresponds to CaMg(CO₃)₂/dolomite (Siligardi et al. 2017), which shows that the native clay or biochar structure is not demolished after the reaction with green nanoparticles. The FTIR spectrum (Fig. S3) shows tetrahedral sheet of Si-O-Si stretching at 470 and 1031 cm⁻¹, Si-O-Al deformation at 526 cm⁻¹, Al-O and Si-O stretching at 693.9 cm⁻¹, Si-O (quartz and silica) deformation at 798 and 779 cm⁻¹, O-H deformation mode of water at 1634 and 3429 cm⁻¹, and vibration of structural O-H group stretching at 3624 cm⁻¹. A wide peak (Fig. S4) at 3440 cm⁻¹ was assigned to the adsorption of water molecules as result of an O-H stretching mode of hydroxyl groups, where the peaks at 2923 and 2852 cm⁻¹ can be attributed to the presence of aliphatic C-H vibration (Zhang et al. 2013; Liu et al. 2018), and then C=O or C=C can be from carboxyl acids (1635 cm⁻¹) (Choudhary et al. 2017) and C-O from carboxylate, at peaks 1435 and 1091 cm⁻¹ (Zhang et al. 2020). After synthesis of BC-gnZVI, some variations can be observed from Fig. S4(b), the -OH group at 3440 cm⁻¹ was tapered and right-shifted to 3375 cm⁻¹. The characteristic peaks at 1640, 1230 and 1065 cm⁻¹ correspond to C=O, C=C,

Fig. 1 SEM images of **a** NC and **b** NC-gnZVI

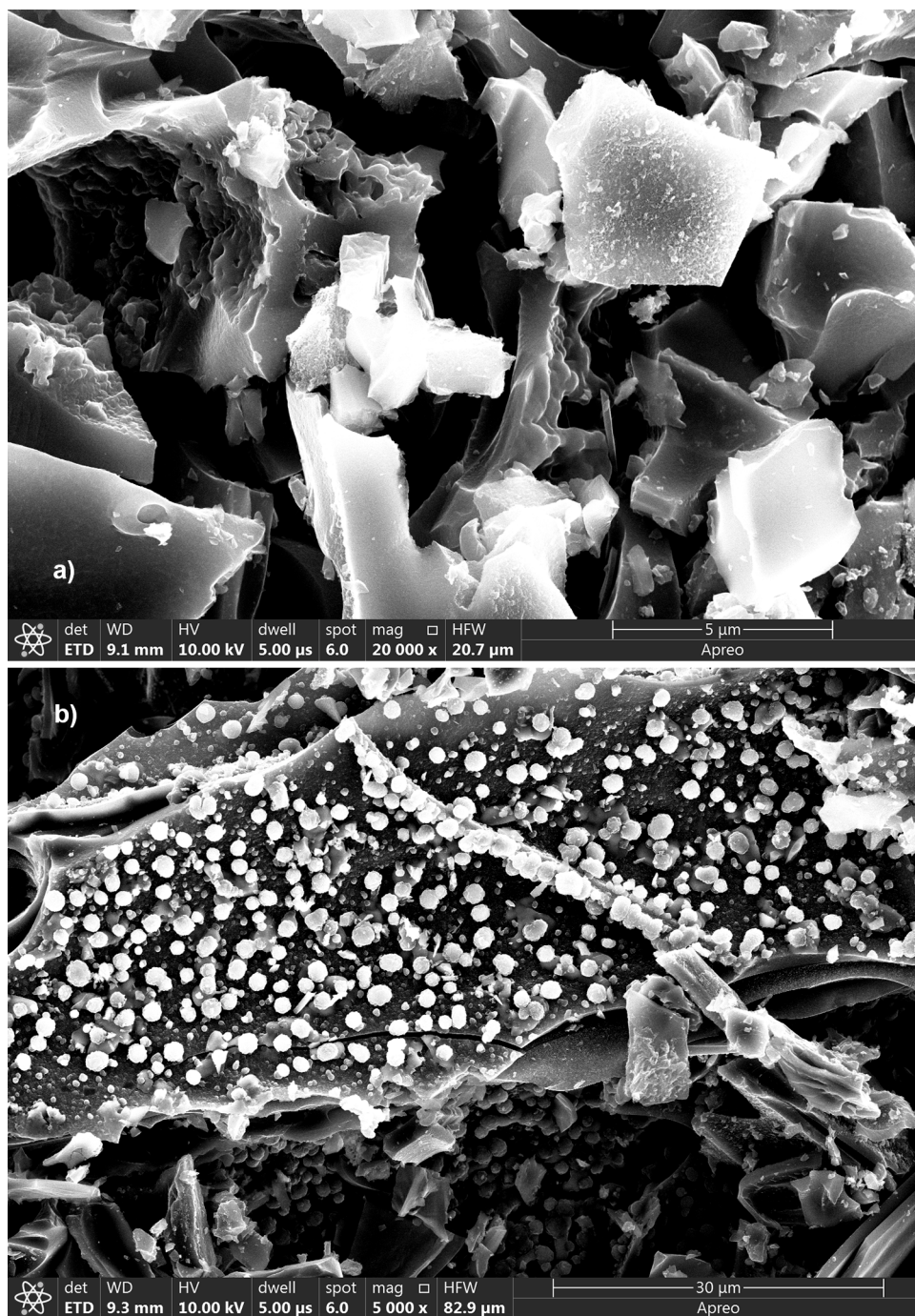


C-N, and C-O (Leng et al. 2015), which indicated that both BC and BC-gnZVI contained plentiful organic functional groups (Liu et al. 2018), and basic chemical composition was not changed by the immobilization of OL-nZVI. The obtained characterization results indicate that green nano Fe(0) particles can be support on native clay or biochar, stable and with minimal agglomeration and that they represent an alternative to chemical synthesis because they act as reducing and stabilizing agents.

4 Characterization of sediment

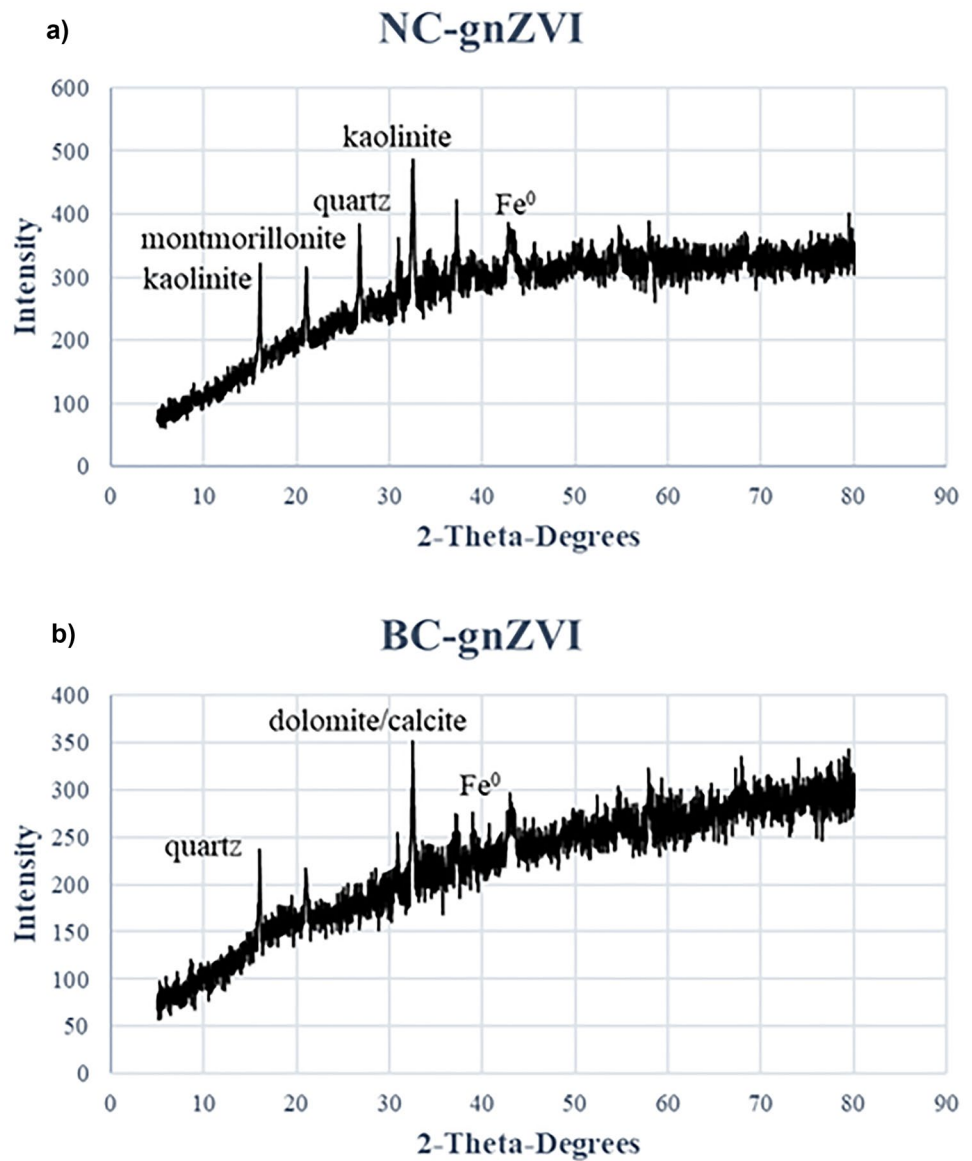
The main characteristic of examined sediment are given in Table S3. The risk assessment of river sediment was determined by Serbian national legal act (“Off. Gazette of RS” No. 50/2012) and given in Table 1. Based on the fact that the quality criteria is given for standard sediment with a content of 10% organic matter and 25% clay, it was necessary to make correction for metals concentrations. For concentration

Fig. 2 SEM images of **a** BC and **b** BC-gnZVI



of PAHs, no correction is necessary. Results for sum of PAH ($2.70 \pm 0.05 \text{ mg kg}^{-1}$) indicate that untreated sediment corresponds to class 2. Class 2 sediments are slightly polluted. A pseudo-total concentration for Cu, Cd, and Ni indicates that sediment corresponds to class 4+. The fourth class according to Serbian legislation classifies the sediment as extremely polluted. For that sediment, there is a need for dredging, or there is a need for different sediment cleanup measures (“Off. Gazette of RS” No. 50/2012).

Stabilization with nanomaterials as remediation technique was used in this study. After the application of nanomaterials as immobilization agents, to evaluate the efficiency of the treatment, leaching and bioavailability tests were used (Fig. S7 Schematic diagram of treatment procedure). The aim of these tests is to simulate the conditions under which the treated mixtures may be exposed if they are disposed in the environment, as well as the classification of the treated sediment as inert, hazardous, or non-hazardous.

Fig. 3 XRD spectra of **a** NC-gnZVI and **b** BC-gnZVI**Table 1** Pseudo-total concentrations of metals and sum of PAHs (mg kg⁻¹)

Parameter	Cu	Cd	Cr	Pb	Ni	Zn	As	Sum of PAHs
	mg kg ⁻¹							
Measured value	312.92 ± 9.02	14.83 ± 0.47	297.63 ± 7.85	477.54 ± 19.10	289.11 ± 8.67	748.42 ± 22.5	62.78 ± 1.06	2.70 ± 0.05
Corrected value	259.15 ± 6.02	12.65 ± 0.26	252.23 ± 5.6	416.53 ± 16.05	229.97 ± 6.54	608.56 ± 18.5	53.58 ± 0.96	-
Target value	36	0.8	100	85	35	140	29	1
Limit value	36	2	380	530	35	480	55	1
Verification level	90	7.5	380	530	45	720	55	10
Remediation value	190	12	380	530	210	720	55	40
Classification	4+	4+	1	1	4+	2	1	2

5 The effectiveness of the stabilization technique from the aspect of metals

5.1 Sequential extraction of an untreated sediment

Sequential extraction was performed in an untreated sediment sample aiming to determine the potential risk of the sediment to the environment. The following decrease in metal mobility can be observed: $Zn > Pb > Cu > Ni > Cd > Cr > As$ (Fig. 4). The difference in percentages in the exchangeable phase for Cu, Cd, Cr, Pb, and Ni is small, but with all the examined metals, their percentage is the highest in the exchangeable phase, which makes them extremely mobile. According to the risk assessment code—RAC (Jain 2004), the percentage of extracted, more easily mobile metals in this phase of extraction ranges from 33.99% for As to 43.74% for Zn of the total metal concentration; thus, this sediment sample is classified as a high-risk category for the environment. A significant percentage of metals are also present in the oxidizable and reducible phases. In the oxidizable fraction, metals are associated with organic components of the sediment, and the immobilization of metals depends on the characteristics of organic matter and the oxidation conditions of the environment. In the reducible fraction, most metals are present above 20% in which the metals bind to iron and manganese (and sometimes aluminum) oxides that would be released if the solid matrix were subjected to anoxic (reduced) conditions, which also makes them potentially mobile. The presence of potentially toxic elements in reducible phase is a consequence from discharging of industrial wastewater into rivers and canals, according to our previous research (Slijepčević et al. 2021).

5.2 Sequential extraction after treatment with nanomaterials

The geochemistry of trace metals in sediment can have an impact on their transport dynamics, as well as on their potential availability to aquatic organisms (Heltai et al. 2018). Based on the results (Fig. 4) of the sequential extraction for all three nanomaterials, the following metals Cu, Cd, Pb, Ni, Zn, and As are the most abundant in the residual fraction in which the metals are occluded in the layers of the crystal lattice of silicates and well-crystallized oxide minerals and are considered the most stable, less reactive, and less bioavailable fraction (Choleva et al. 2020). Percentages of metals found in this fraction for all three nanomaterials were above 50% and are not expected to be released into the solution under conditions encountered in nature. The treatment of sediment with 5%wt BC-gnZVI was more successful in terms of As (94%), Pb (66%), Cd (57%), and Cu (76%). However, very small differences were observed in the application of these three amendments as immobilization agents of the contaminated sediment. The results show that organic matter has a stronger geochemical affinity for chromium, which leads to the formation of organic complexes and a higher percentage of this metal in the oxidizable fraction (Choleva et al. 2020). If conditions are changed and the degradation of organic matter is happened, then it can point to the release and to the leaching of bound metals from this fraction in the sediment (Choleva et al. 2020). These changes in metal speciation suggest that sediment treatment using green synthesized nZVI from the oak leaf extract and also supported by native clay and bio-char has had results in the mitigation of direct toxicity and in reduction of potential environmental risk.

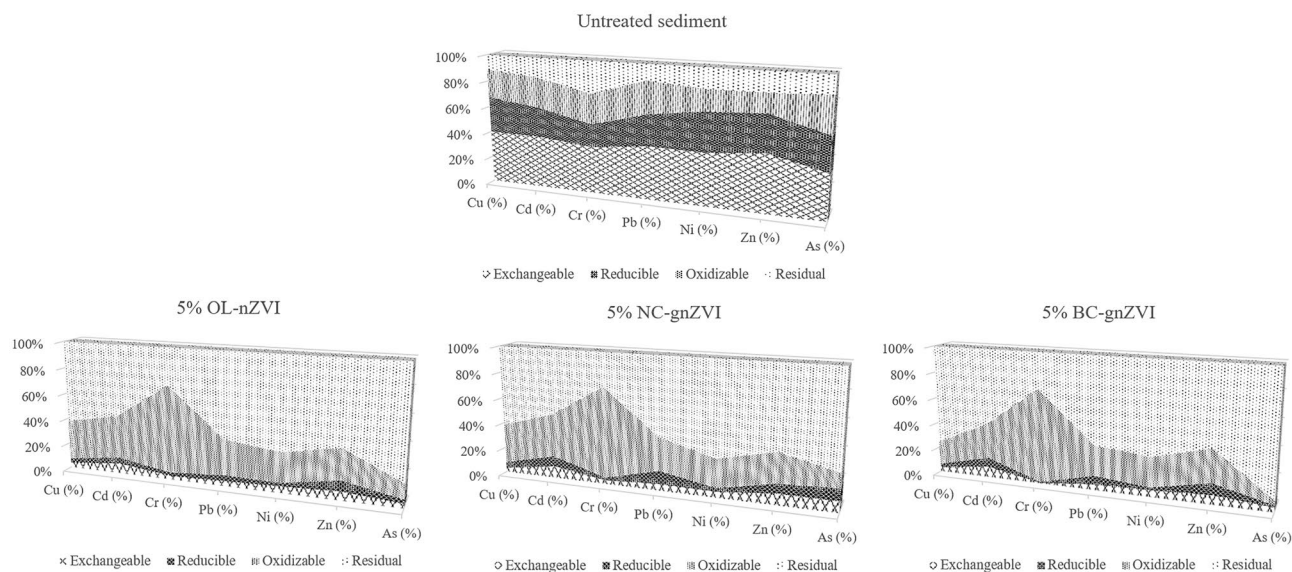


Fig. 4 Sequential extraction (%) before and after the treatment

The risk assessment established on the percentage of metals in the exchangeable (carbonate) fraction of the sediment confirms that none of the examined metals represents a risk to aquatic systems, as their values have been below 10% (Jain 2004). Comparing the percentage shares of the examined metals in the sediment which were treated with green nano zero-valent iron, their significant reduction in the exchangeable and in the reducible fraction is observed in relation to the untreated sediment. The results presented in Fig. 4 provide a useful guide in assessing the long-term potential risk of potentially toxic elements in the environment.

5.3 Assessment of the metal bioavailability using HCl, EDTA and the first phase of BCR

Bioavailability with hydrochloric acid and EDTA is certainly a faster and an easier method for determining the current state of the sediment quality. Comparing the results of the first phase of sequential extraction (acetic acid has been used as an extraction agent) and bioavailability with HCl and EDTA shown in Fig. S5(a–c), we can conclude that the leached concentrations of potentially toxic elements are higher with the use of HCl and with the use of EDTA just in case of Cu, Pb, and Zn. These three metals have deep affinity for Fe oxides and hydroxides and can be remobilized because of the complexation of Fe with EDTA ($\log K = 25.1$). (Žemberyová et al. 2007). Compared with HCl, EDTA ligand has had less capacity to remove acid extractable and reducible Cu and Zn. On other hand, it has had great ability to remove the oxidizable Cu than Zn (Wang et al. 2017). Based on the presented results (Fig. S5), in sediment mixtures with 5%wt OL-nZVI, 5%wt NC-gnZVI, and 5%wt BC-gnZVI, we can observe higher percentages (72–82%) of chromium leaching in comparison with other examined potentially toxic elements, which we can attribute to the acidic characteristics and chelating properties of Cl^- (Wang et al. 2017). Acetic acid, as a weak acid, is used to simulate the effects of the input of acidic properties (through acid rain or accidental low-pH spills or discharges) to the sediment (Wang et al. 2017). Therefore, it is normal to expect that the first phase of sequential extraction contains easily mobile and bioavailable metal fractions, which are released into the solution with a slight change in the pH value of the sediment. In the case of stronger acids, such as HCl, under the influence of H^+ attack, the destruction of hydro(oxides) in the sediment occurs, which are primarily hosts of metal ions, which demonstrates the greater capacity of the HCl solution to remove/leach metals from the sediment. EDTA was also proved to be very adequate organic ligand in mobilizing solid-bound metals (Leleyter et al. 2012), due to its strong attracting abilities for potentially toxic

elements (Shahid et al. 2014) via direct complexation and indirect dissolution of reducible and oxidizable sediment components (Wang et al. 2017).

5.4 Assessment of toxic characteristic using one step extraction tests

To test the effectiveness of S/S treatment based on leached concentrations of potentially toxic elements, the TCLP leaching test was applied, in order to characterize waste as hazardous or non-hazardous. In all three mixtures (Table S4), the obtained results do not exceed the limit values according by Serbian regulations (Official Gazette 56/2010) and those set by the EPA (40 CFR Parts 261 2005). Therefore, it can be concluded that the three mixtures do not have toxic characteristics and such waste is considered non-hazardous in terms of leached concentrations of Cu, Cd, Cr, Pb, Ni, Zn, and As. The obtained pH values after applied extraction were from 7.13 and 7.16 to 7.18 pH units for 5%wt OL-nZVI, 5%wt NC-gnZVI, and 5%wt BC-gnZVI, respectively, which is in accordance with the prescribed values when disposing of such treated waste/sediment at sanitary landfills. The German standard leaching test (DIN 38414–4) simulates real conditions in nature, using deionized water as a leaching agent. Based on the obtained concentrations (Table S5) of Cu, Cd, and Zn, all three mixtures are classified as inert waste, while from the aspect of the leached concentrations of Cr and Ni, it represents a non-hazardous waste. Other two metals (Pb and As) have different classification, based on concentrations of Pb, mixture with 5% OL-nZVI has been considered inert waste, but other two mixtures have exceeded values for waste which is considered as (Table S5). If we observe concentrations of As, only mixture with 5% NC-gnZVI has exceeded the limit value of inert waste. This mixture does not exhibit toxic effects and can be disposed of safely, as it is considered as non-hazardous waste based on the all above criteria. The pH values for all mixtures (8.22; 8.30; 8.26) are in accordance with the prescribed values, while the leached solutions have showed slightly alkaline properties. The results from both leaching tests are in good agreement with mentioned above conclusions from sequential extraction, that after treatment with nanomaterials, metals are safely stabilized with leaching concentrations below 10% (Table S6) of total metals from mixtures and thus do not represent a threat during disposal of mixtures into the environment. After conducting the TCLP test, the lowest percentage was observed in the mixture containing 5% BC-gnZVI (0.42%), while the highest percentage was found in the mixture with 5% NC-gnZVI. In the case of the DIN test, the lowest percentage was observed with 5% OL-nZVI (0.20%), and again, the highest was recorded with 5% NC-gnZVI (1.65%).

5.5 Removal mechanisms of potentially toxic elements with green iron nanoparticles

The final valence state and the main mechanism for heavy metal removal are related to the standard redox potential (E^0). The mechanism between nano zero-valent iron and potentially toxic elements mainly involves adsorption, reduction and precipitation/co-precipitation (Fig. 5).

When the redox potential of the metal is much higher (positive) than the redox potential of iron, the metal is generally removed through reduction, such as Cu(II). When the redox potential of the metal is lower (negative) or close to Fe^0 , the metal is mainly removed by adsorption, such as Zn(II), Cd(II), and As(V). In the case when the redox potential of the metal is slightly higher (positive) than the redox potential of iron, the metal can be removed by the dual effects of adsorption and reduction (for example, Pb(II), Ni(II), and Cr(VI)) (Huang et al. 2017). The native clay used in this work to stabilize iron nanoparticles behaves as a chelating agent for potentially toxic elements and also for $Fe(0)$ nanoparticles, which is in good correlation with the BET specific surface area of native clay previously mentioned and shown in papers by Soliemanzadeh and Fekri (2017), Tomašević Pilipović et al. (2018), Slijepčević et al. (2018), Ye et al. (2021), and Yang et al. (2021). Although supports with native clay have showed good results, there

are some disadvantageous due to the complications of separation, recovery, and less ability for reactions with organic pollutants (Wang et al. 2019a). Carbonaceous materials like used biochar have excellent reactivity with potentially toxic elements or organic pollutants and thus supply green nano zero-valent iron with higher catalytic capacity. BC also supplies nZVI with suitable matrix (with pores, and large SA) to lodge nZVI particles (Wang et al. 2019a). Removal mechanism of potentially toxic elements by BC-gnZVI includes ion exchange, electrostatic attraction, surface complexation, and π - π interactions (Dong et al. 2011). Removal by BC-gnZVI can be refer to role of oxygen atoms in the O-H groups and C=O of BC and the Fe-O groups of nZVI that may form coordination complexes with metal ions by addition pairs of free electrons (Yang et al. 2018). In a few studies, surface complexation of Pb, Cu, and Zn was validated (Diao et al. 2018; Yang et al. 2018). Knowing that BCs are described by high point of zero charge values, these properties also support electrostatic attraction with anionic HMs, governing to the design of inner-sphere complexes. BC also provide active surface sites for the removal of HMs by redox reactions (Wang et al. 2019a). Su et al. (2016) has found that biochar and ZVI have symbiotic effects on the immobilization of Cd(II) and As(V) from solid matrixes. In another study (Qiao et al. 2018), use of nZVI (0.4%) and nZVI/BC (0.8%) has immobilized about 100% Cr(VI) from soil.

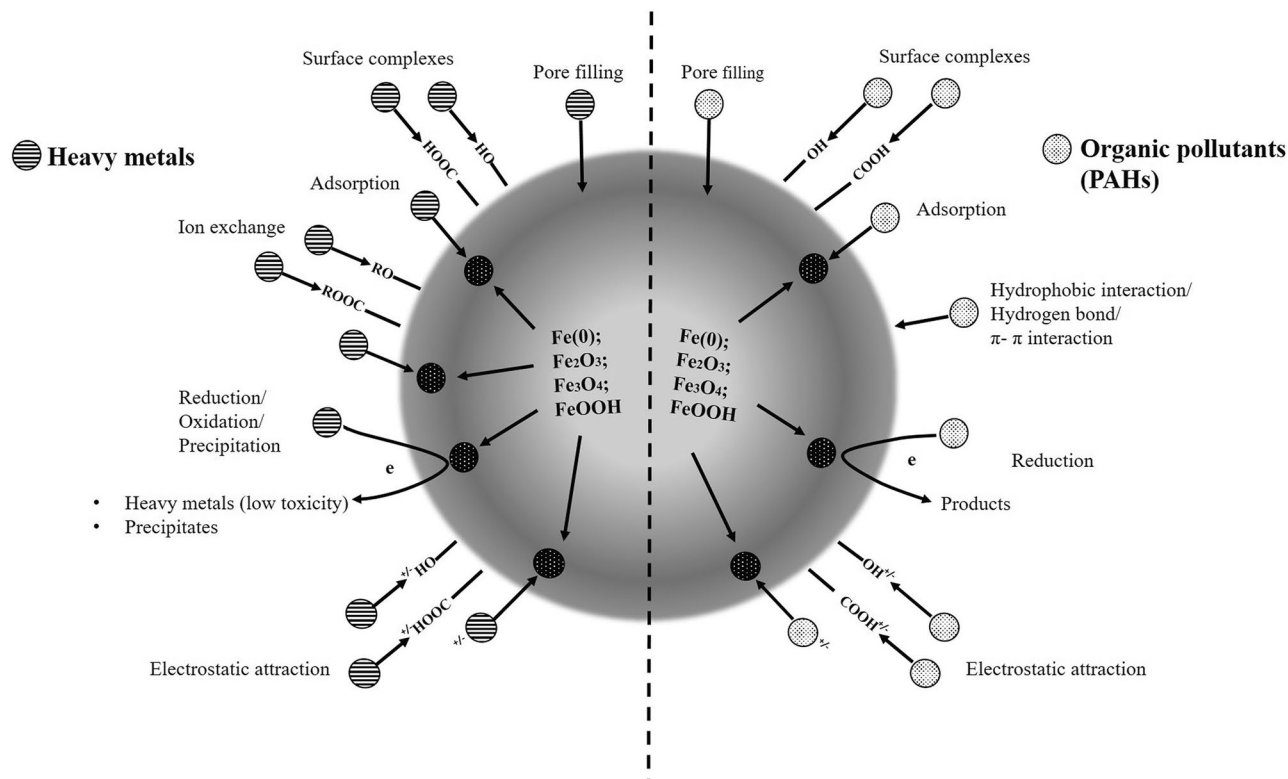


Fig. 5 The removal mechanisms of metals and PAHs

6 The effectiveness of the stabilization technique from aspect of PAHs

6.1 The estimation of the bioaccessible fraction of PAH in an untreated sediment

The initial concentrations of PAHs in untreated sediment sample were in range of 6.09 ± 0.22 for acenaphthylene to $393.78 \pm 12.3 \mu\text{g kg}^{-1}$ for pyrene (Table 2). Low-molecular-weight/high-molecular-weight ratio were used for the description of sediment pollution source (Kuppusamy et al. 2017). $\text{LMW}_{\text{PAH}}/\text{HMW}_{\text{PAH}}$ in the untreated sediment sample was 0.08 indicating a pyrogenic source for the PAHs present. In the literature (Han et al. 2019), for more information about potential sources of PAHs, the most commonly used are ratios including Flu/(Flu + Py) and Ant/(Ant + Phe). The first ratio was 0.49 and the second 0.38 which suggesting that fuel combustion (Flu/(Flu + Py) in range 0.4–0.5) and pyrogenic (Ant/(Ant + Phe) > 0.1) as the main sources. The combustion origin is most likely from liquid fossil fuel from river sediment activities. In the current study, XAD-4 extraction was used for indicating bioavailable fraction in untreated sediment sample. Results (Table 2) show that the sum of the stripped/desorbed PAHs was 3.30% of all total PAHs in the untreated sediment sample.

Cui et al. (2013) state that this extraction technique can be good predictors for bioavailability of PAHs which contains octanol/water partition coefficient (K_{ow}) values < 6.0. In Posada-Baquero et al. (2019), a recommendation was given that the single time point can be a reliable tool for bioavailability assessment.

6.2 Total content and bioavailability of PAHs after sediment treatment with nanomaterials

The content of PAHs after stabilization of the sediment sample with 5%wt OL-nZVI, 5%wt NC-gnZVI, 5%wt BC-gnZVI, and after 24 h of extraction with XAD-4 resin was represented in Table 3.

The ratio between LMW_{PAH} and HMW_{PAH} and Flu/(Flu + Py) and Ant/(Ant + Phe) remained the same as in the untreated sediment. Although the mentioned ratios stay the same, the concentrations as we can see in Table 3 were decreased compared to the beginning. These three sediment mixtures based on concentrations for sum of PAHs belong to class 0 where sediments are at the level of non-pollution. The percentage of desorbed PAHs after 24 h of extraction with XAD-4 resin was slightly higher than in the untreated sample, for mixture of 5%wt OL-nZVI 7.6%, 5%wt NC-gnZVI 9.8%, and 5%wt BC-gnZVI 9.5% (Fig. S6). This could have been caused by the percentage of organic matter, by the proportion of biochar and clay as supporting agents and by the reaction of PAHs with them. Individual concentrations for PAHs after extractions in all three mixtures were smaller, indicating that there was still less bioavailability of PAHs after sediment stabilization. For example, concentration of phenanthrene in untreated sediment sample was $80.65 \mu\text{g kg}^{-1}$, and after the treatment with 5%wt OL-nZVI, it was $80.59 \mu\text{g kg}^{-1}$; with 5%wt NC-gnZVI, it was $77.91 \mu\text{g kg}^{-1}$, and with 5%wt BC-gnZVI, it was $74.50 \mu\text{g kg}^{-1}$. If we observe concentrations after 24 h of extraction with XAD-4 resin, then these concentrations have been 27.13, 16.16, 19.49, and $16.09 \mu\text{g kg}^{-1}$, respectively. A

Table 2 PAH concentration ($\mu\text{g kg}^{-1}$) in untreated sediment sample before (start) and after single step extraction (24 h XAD-4) with resin XAD-4

Analyzed PAHs	Number of rings	Start	24 h XAD-4	Log K_{ow}
Naphthalene	2	31.48 ± 1.13	0.19 ± 0.01	3.32
Acenaphthylene	3	6.09 ± 0.22	1.14 ± 0.05	3.93
Acenaphthene	3	9.02 ± 0.25	0.30 ± 0.01	4.33
Fluorene	3	32.45 ± 0.99	0.51 ± 0.01	4.18
Phenanthrene	3	80.65 ± 3.22	27.13 ± 0.44	4.57
Anthracene	3	49.08 ± 1.15	11.44 ± 0.22	4.54
Fluoranthene	4	371.75 ± 10.5	14.85 ± 0.22	5.18
Pyrene	4	393.78 ± 12.3	13.38 ± 0.22	5.22
Chrysene	4	311.07 ± 11.6	6.97 ± 0.13	5.91
Benzo(a)anthracene	4	307.49 ± 10.8	6.65 ± 0.15	5.91
Benzo(b)fluoranthene+	5	607.73 ± 15.2	3.86 ± 0.12	5.80/5.90
Benzo(k)fluoranthene	5			
Benzo(a)pyrene	5	78.82 ± 2.66	3.49 ± 0.12	6.00
Dibenzo(a, h)anthracene+	5	221.24 ± 3.65	0.00	6.75/6.50
Indeno (1,2,3 cd) pyrene	6			
Benzo(g,h,i)perylene	6	199.67 ± 2.82	0.00	6.50
Sum PAH	-	2700.32 ± 50	89.91 ± 3.52	-

Table 3 PAH concentration ($\mu\text{g kg}^{-1}$) in sediment mixtures with nanomaterials before (start) and after single step extraction (24 h XAD-4) with resin XAD-4

Mixtures Analyzed PAHs	5%wt OL-nZVI		5%wt NC-gnZVI		5%wt BC-gnZVI	
	Start	24 h XAD-4	Start	24 h XAD-4	Start	24 h XAD-4
Naphthalene	28.33 ± 1.13	1.40 ± 0.05	25.33 ± 0.12	1.42 ± 0.05	23.53 ± 1.15	0.39 ± 0.02
Acenaphthylene	1.14 ± 0.05	0.03 ± 0.01	1.44 ± 0.05	0.08 ± 0.01	1.50 ± 0.05	0.15 ± 0.01
Acenaphthene	3.99 ± 0.12	0.83 ± 0.01	7.50 ± 0.22	0.13 ± 0.01	6.03 ± 0.15	0.13 ± 0.01
Fluorene	18.49 ± 0.16	0.75 ± 0.01	23.07 ± 1.20	2.98 ± 0.11	25.48 ± 1.07	4.11 ± 0.20
Phenanthrene	80.59 ± 3.22	16.16 ± 0.30	77.91 ± 3.03	19.49 ± 0.22	74.50 ± 1.88	16.09 ± 0.80
Anthracene	25.67 ± 1.25	4.50 ± 0.11	30.88 ± 1.13	8.06 ± 0.32	32.76 ± 1.22	6.74 ± 0.34
Fluoranthene	107.36 ± 4.29	10.25 ± 0.33	95.02 ± 2.85	12.70 ± 0.12	88.05 ± 2.64	11.20 ± 0.15
Pyrene	105.15 ± 3.66	9.55 ± 0.29	92.97 ± 3.30	11.65 ± 0.12	89.18 ± 2.43	10.49 ± 0.15
Chrysene	73.18 ± 2.88	3.58 ± 0.10	62.71 ± 2.16	4.32 ± 0.13	70.40 ± 2.10	3.82 ± 0.12
Benzo(a)anthracene	74.58 ± 2.90	3.57 ± 0.11	63.69 ± 2.06	4.29 ± 0.10	69.48 ± 2.07	3.67 ± 0.12
Benzo(b)fluoranthene+	168.71 ± 4.03	2.91 ± 0.10	143.29 ± 3.88	3.28 ± 0.09	157.11 ± 3.62	3.32 ± 0.12
Benzo(k)fluoranthene						
Benzo(a)pyrene	17.15 ± 0.32	0.31 ± 0.02	21.71 ± 1.10	0.37 ± 0.03	15.46 ± 0.23	1.87 ± 0.03
Dibenzo(a, h)anthracene+	0.00	0.00	0.00	0.00	0.00	0.00
Indeno (1,2,3 cd) pyrene						
Benzo(g,h,i)perylene	0.00	0.00	58.95 ± 2.62	0.00	0.00	0.00
Sum PAH	704.34 ± 28.2	53.83 ± 2.80	704.46 ±	68.78 ± 2.74	653.47 ± 26.1	62.00 ± 1.88

similar trend is noticeable with other PAH compounds. Bio-availability of PAHs as the potential factor of successively reducing the nZVI application was excluded (Oleszczuk and Koltowski 2017), because its weak removal of PAHs could have been by the constraining activity of nZVI in a complex compound such as sediment.

6.3 Removal mechanisms of PAHs with green iron nanoparticles

According to the above discussions and Fig. 5, it can be established that the removal mechanism of organic pollutants and nZVI are mainly under the influence of the following: (1) adsorption and coprecipitation with iron oxide/oxyhydroxide; (2) redox reactions on nZVI surface; and (3) fabrications of ionic species (free radicals) in order to chemically degrade organic pollutants (Li et al. 2021). The one of the most essential processes for organic pollutants removal is adsorption. Two steps are included in the adsorption, i.e., the first appear individually on the surface of oxidation coat of nZVI or on its compounds. The synergistic effect is referred to by the second step between the supporting porous material (such as native clay/biochar in this research) and nZVI (Li et al. 2021). The reduction has also got a prominent role thanks to core-shell structure of green nZVI which is provided by the reductive properties of Fe^0 and Fe^{2+} (Ahmed et al. 2017). The hydrogenation, hydrogenolysis, and coupling processes are the reduction processes which appear (He et al. 2018). Green synthesis of nanomaterials was applied in order to remove

organic pollutants like in research Hassan et al. (2018) (using pomegranate peel extract for production of nanoparticles) and also by Rani and Shanker (2018), Husen and Iqbal (2019), Sivodia and Sinha (2022), and Mirzaee and Sartaj (2023). The removal of organic pollutants by BC-gnZVI is attributed also to the adsorption process, reductive/catalytic and mass transfer capacities of biochar, and its synergy with nZVI (Wang et al. 2019a). Organic molecules from (poly)aromatic and aliphatic compounds can be mainly adsorbed and then by hydrophobic and electron attraction processes between BC surface and organic pollutants and diffusion through the pores of biochar. In recent studies, it was found that BC-nZVI treatments have decreased the content of PAH by more than 82% (Oleszczuk and Koltowski 2017). Although the PAHs were adsorbed by sorptive sites onto biochar surface and they are less available, the existence of biochar in the soil/sediment can enhance the number of microorganisms in solid matrixes and encourage degradation of PAHs, decreasing the half-lives of PAHs in solid matrixes (Kusmierz et al. 2016).

7 The impact of the simultaneous presence of contaminants (potentially toxic elements and PAHs) in the sediment

Based on the results and discussion mentioned above, special attention should be paid on reaction mechanism for the stimulations removal of potentially toxic elements

and PAHs and on the influence of environmental factors on removal efficiency (Fig. 5). This removal takes part in the direct reduction by Fe^0 and also in both adsorption and co-precipitation (Kang et al. 2018) by iron(hydro)oxides or biochar and native clay. For example, Liu et al. (2018) investigated the mechanism of Cu^{2+} and BPA (bisphenol A) removal, where first Cu^{2+} was adsorbed on the surface of BC-nZVI (BPA also is partially adsorbed). Then, it was co(precipitated) with carboxyl and hydroxyl groups, and subsequently, it was reduced to Cu^0 whereby Fe^{2+} would be released under acidic conditions and would activate the removal of BPA by presence of surfactants like persulfate (PS). The use of surfactants in the removal of pollutants has few limitations, including that they are readily biodegradable, as well as massive quantities of surfactants could have serious effects on the ecosystem. The pH factor and organic matter can affect nZVI performance by increasing the solubility of organic pollutants, which form complexes with metals and other organic pollutants, thereby impacting the passivation of nZVI (Zhao et al. 2016). Biochar itself can also contribute to the additional amount of carbon, which can have negative or positive influence on the sediment organic matter (Zimmerman et al. 2011). Due to their characteristics, particular pollutants can be antagonistic to, or coactive with, or neutral with tribute to the target pollutants. For example, neutral organic composites were not affected to the glyphosate removal, but they were raised by metal which formed inner-sphere structures with the carboxyl groups of biochar and hydroxyl groups of Fe oxides (Wang et al. 2019b). Some cationic potentially toxic elements have different affinities for sorption sites, and some sorption sites surface on nZVI were blocked by newly formed metal-hydroxides or compounds (Wang et al. 2010). Unfortunately, their simultaneous removal is not as simple as a single or a specific contaminant removal. Looking ahead, research about antagonistic effect of one pollutant over another should be aimed to ways of minimizing it, because numerous organic pollutants and potentially toxic elements co-exist already in the environment causing serious toxicological residues (Ajiboye et al. 2021).

8 Conclusion

The present study showed that co-application of supported material like native clay and biochar with green nano zero-valent iron synthesized from oak leaves extract and iron(III)salt are promising material for simultaneous immobilization of PAHs and potentially toxic elements in sediment. These nanomaterials (NC-gnZVI and BC-gnZVI) successfully showed good dispersion on native clay or biochar surface by SEM/EDS, TEM, XRD, FTIR, and BET methods, while not affecting the structure of

supported materials. It was clearly demonstrated that removal of potentially toxic elements was better than removal of PAHs, because all metals across from mobile/available phase to residual good stabilized phase in sediment matrix, where they do not pose a threat to the environment. Certainly, the concentrations of PAHs were also low in the initial sediment sample, but even on this basis, the removal after remediation using NC and BC-gnZVI was noticeable. Future work should focus on (i) immobilization of sediment in different mass proportion of supported native clay and biochar nZVI, because in this study it showed only 5%wt; (ii) potential toxicity of nanomaterials; (iii) how supported material effects on the long-term effectiveness of green nZVI; and (iv) how to established maximum removal capacity for organic and inorganic contaminants. Developing the green nZVI procedures has been improved over the last few years. However, new pathways have to be implemented in order to achieve circular economy goals. Production of nZVI and his modification represent a challenge; therefore, science must response with reduction of the cost of synthesis and by expanding the possibility of applying these nanomaterials.

Supplementary Information The online version contains supplementary material available at <https://doi.org/10.1007/s11368-023-03682-w>.

Author contribution NS: investigation; writing, original draft; conceptualization. DR: methodology, visualization, supervision, writing—review and editing. JB: methodology, formal analysis. GK: data curation, formal analysis. ZK: data curation, formal analysis, writing—review and editing. SM: methodology, writing — review and editing. DTP: writing, review and editing; resources, project administration, funding acquisition.

Funding The research was financed by the Science Fund of the Republic of Serbia, #7753609, BEuSED.

Declarations

Conflict of interest The authors declare no competing interests.

References

- Ahmad S, Liu X, Tang J, Zhang S (2022) Biochar-supported nano-sized zero-valent iron (nZVI/BC) composites for removal of nitro and chlorinated contaminants. *J Chem Eng* 431(4):133187. <https://doi.org/10.1016/j.cej.2021.133187>
- Ahmed MB, Zhou JL, Ngo HH, Guo W, Johir MAH, Sornalingam K, Belhaj D, Kallel M (2017) Nano-Fe0 immobilized onto functionalized biochar gaining excellent stability during sorption and reduction of chloramphenicol via transforming to reusable magnetic composite. *J Chem Eng* 322:571–581. <https://doi.org/10.1016/j.cej.2017.04.063>
- Ajiboye TO, Oyewo OA, Onwudiwe DC (2021) Simultaneous removal of organics and heavy metals from industrial wastewater: a review. *Chemosphere* 262:128379. <https://doi.org/10.1016/j.chemosphere.2020.128379>

- ASTM D1557–00 Standard test method for laboratory compaction characteristics of soil using modified effort American Society for Testing Materials. Annual book of ASTM standards: ASTM D1557–91:4.08. ASTM, Philadelphia
- Choleva TG, Tsogas GZ, Vlessidis AG, Giokas DL (2020) Development of a sequential extraction and speciation procedure for assessing the mobility and fractionation of metal nanoparticles in soils. *Environ Pollut* 263 (PartA):114407. <https://doi.org/10.1016/j.envpol.2020.114407>
- Choudhary B, Paul D, Singh A, Gupta T (2017) Removal of hexavalent chromium upon interaction with biochar under acidic conditions: mechanistic insights and application. *Environ Sci Pollut Res* 24(20):16786–16797. <https://doi.org/10.1007/s11356-017-9322-9>
- Cornelissen G, Van Noort PCM, Govers HAJ (1997) Desorption kinetics of chlorobenzenes, polycyclic aromatic hydrocarbons, and polychlorinated biphenyls: sediment extraction with Tenax and effects of contact time and solute hydrophobicity. *Environ Toxicol Chem* 16:1351–1357. <https://doi.org/10.1002/etc.5620160703>
- Cui X, Mayer P, Gan J (2013) Methods to assess bioavailability of hydrophobic organic contaminants: principles, operations, and limitations. *Environ Pollut* 172:223–234. <https://doi.org/10.1016/j.envpol.2012.09.013>
- Diao ZH, Chu W (2021) FeS₂ assisted degradation of atrazine by bentonite-supported nZVI coupling with hydrogen peroxide process in water: performance and mechanism. *Sci Total Environ* 754:142155. <https://doi.org/10.1016/j.scitotenv.2020.142155>
- Diao ZH, Du JJ, Jiang D, Kong LJ, Huo WY, Liu CM, Wu QH, Xu XR (2018) Insights into the simultaneous removal of Cr⁶⁺ and Pb²⁺ by a novel sewage sludge-derived biochar immobilized nanoscale zero valent iron: coexistence effect and mechanism. *Sci Total Environ* 642:505–515. <https://doi.org/10.1016/j.scitotenv.2018.06.093>
- DIN 38414–4 (1984) Teil 4: Schlamm und Sedimente, Gruppe S., Bestimmung der Eluierbarkeit mit Wasser S4, Beuth Verlag, Berlin
- Dong X, Ma LQ, Li Y (2011) Characteristics and mechanisms of hexavalent chromium removal by biochar from sugar beet tailing. *J Hazard Mater* 190(1–3):909–915. <https://doi.org/10.1016/j.jhazmat.2011.04.008>
- EBC (2012–2022) European biochar certificate - guidelines for a sustainable production of biochar. European Biochar Foundation (EBC), Arbaz, Switzerland
- EPA (2004) The incidence and severity of sediment contamination in surface waters of the United States. Second Edition, National Sediment Quality Survey
- Francy N, Shanthakumar S, Chiampo F, Sekhar YR (2020) Remediation of lead and nickel contaminated soil using nanoscale zero-valent iron (nZVI) particles synthesized using green leaves: first results. *Processes* 8:1453. <https://doi.org/10.3390/pr8111453>
- Guo J, Yin Z, Zhong W, Jing C (2022) Immobilization and transformation of co-existing arsenic and antimony in highly contaminated sediment by nano zero-valent iron. *J Environ Sci* 112:152–160. <https://doi.org/10.1016/j.jes.2021.05.007>
- Han B, Zheng L, Lin F (2019) Risk assessment and source apportionment of PAHs in surface sediments from Caofeidian Long Island, China. *Mar Pollut Bull* 145:42–46. <https://doi.org/10.1016/j.marpolbul.2019.05.007>
- Hassan SSM, Abdel-Shafy HI, Mansour MSM (2018) Removal of pyrene and benzo(a)pyrene micropollutant from water via adsorption by green synthesized iron oxide nanoparticles. *Adv Nat Sci: Nanosci Nanotechnol* 9(1):015006. <https://doi.org/10.1088/2043-6254/aaa6f0>
- He F, Li ZJ, Shi SS, Xu WQ, Sheng HZ, Gu YW, Jiang YH, Xi BD (2018) Dechlorination of excess trichloroethene by bimetallic and sulfidated nanoscale zero-valent iron. *Environ Sci Technol* 52:8627–8637. <https://doi.org/10.1021/acs.est.8b01735>
- Heltai G, Györi Z, Fekete I, Halász G, Kovács K, Takács A, Boros N, Horváth M (2018) Long-term study of transformation of potentially toxic element pollution in soil/water/sediment system by means of fractionation with sequential extraction procedures. *Microchem J* 136:85–93. <https://doi.org/10.1016/j.microc.2017.01.026>
- Huang X, Wang W, Ling L, Zhang W (2017) Heavy metal-nZVI reactions: the core-shell structure and applications for heavy metal treatment. *Acta Chimica Sinica -Chinese Edition* 75(6):529. <https://doi.org/10.6023/A17020051>
- Husen A, Iqbal M (2019) Nanomaterials and plant potential: an overview. In: Husen A, Iqbal M (eds) *Nanomaterials and Plant Potential*. Springer, Cham
- ISO 565:1990 Test sieves - metal wire cloth, perforated metal plate and electroformed sheet - nominal sizes of openings
- ISO 11464:2006 Soil quality—pretreatment of samples for physico-chemical analyses
- ISO 11277:2009 Soil quality-determination of particle size distribution in mineral soil material-method by sieving and sedimentation.
- Jain CK (2004) Metal fractionation study on bed sediments of River Yamuna, India. *Water Res* 38:569–578. <https://doi.org/10.1016/j.watres.2003.10.042>
- Jamali MK, Kazi TG, Arain MB, Afridi HI, Jalbani N, Kandhro GA, Shah AQ, Baig JA (2009) Speciation of heavy metals in untreated sewage sludge by using microwave assisted sequential extraction procedure. *J Hazard Mater* 163:1157–1164. <https://doi.org/10.1016/j.jhazmat.2008.07.071>
- Kang YG, Yoon H, Lee W, Kim E-j, Chang Y-S (2018) Comparative study of peroxide oxidants activated by nZVI: removal of 1,4-dioxane and arsenic(III) in contaminated waters. *J Chem Eng* 334:2511–2519. <https://doi.org/10.1016/j.cej.2017.11.076>
- Kecić V, Kerkez Đ, Prica M, Luzanin O, Bečelić-Tomin M, Tomasević Pilipović D, Dalmacija B (2018) Optimization of azo printing dye removal with oak leaves nZVI/H₂O₂ system using statistically designed experiment. *J Clean Prod* 202:65–80. <https://doi.org/10.1016/j.jclepro.2018.08.117>
- Kerkez Đ, Tomašević D, Kozma G, Bečelić-Tomin M, Prica M, Rončević S, Kukovec A, Dalmacija B, Konya Z (2014) Three different clay-supported nanoscale zero-valent iron materials for industrial azo dye degradation: a comparative study. *J Taiwan Inst Chem Eng* 45(5):2451–2461. <https://doi.org/10.1016/j.jtice.2014.04.019>
- Krčmar D, Dubovina M, Grba N, Pešić V, Watson M, Tričković J, Dalmacija B (2017) Distribution of organic and inorganic substances in the sediments of the “Great Bačka Canal”, a European environmental hotspot. *Sci Total Environ* 601:833–844. <https://doi.org/10.1016/j.scitotenv.2017.05.251>
- Kuppusamy S, Thavamani P, Venkateswarlu K, Lee YB, Naidu R, Megharaj M (2017) Remediation approaches for polycyclic aromatic hydrocarbons (PAHs) contaminated soils: technological constraints, emerging trends and future directions. *Chemosphere* 168:944–968. <https://doi.org/10.1016/j.chemosphere.2016.10.115>
- Kusmierz M, Oleszczuk P, Kraska P, Palys E, Andruszczak S (2016) Persistence of polycyclic aromatic hydrocarbons (PAHs) in biochar-amended soil. *Chemosphere* 146:272–279. <https://doi.org/10.1016/j.chemosphere.2015.12.010>
- Lakkaboyana SK, Khantong S, Asmel NK, Obaidullah S, Kumar V, Kannan K, Venkateswarlu K, Yuzir A, Yaacob WZW (2021) Indonesian Kaolin supported nZVI (IK-nZVI) used for the an efficient removal of Pb(II) from aqueous solutions: kinetics, thermodynamics and mechanism. *J Environ Chem Eng* 9(6):106483. <https://doi.org/10.1016/j.jece.2021.106483>
- Leleyter L, Rousseau C, Biree L, Baraud F (2012) Comparison of EDTA, HCl and sequential extraction procedures, for selected metals (Cu, Mn, Pb, Zn), in soils, riverine and marine sediments. *Geochem Explor* 116–117:51–59. <https://doi.org/10.1016/j.gexplo.2012.03.006>

- Leng LJ, Yuan XZ, Huang HJ, Shao JG, Wang H, Chen XH, Zeng GM (2015) Biochar derived from sewage sludge by liquefaction: characterization and application for dye adsorption. *Appl Surf Sci* 346:223–231. <https://doi.org/10.1016/j.apsusc.2015.04.014>
- Li X, Huang L, Fang H, He G, Reible D, Wang C (2019) Immobilization of phosphorus in sediments by nano zero-valent iron (nZVI) from the view of mineral composition. *Sci Total Environ* 694:133695. <https://doi.org/10.1016/j.scitotenv.2019.133695>
- Li Z, Wang L, Wu J, Xu Y, Wang F, Tang X, Xu J, Sik Ok Y, Meng J, Liu X (2020) Zeolite-supported nanoscale zero-valent iron for immobilization of cadmium, lead, and arsenic in farmland soils: encapsulation mechanisms and indigenous microbial responses. *Environ Pollut* 260:114098. <https://doi.org/10.1016/j.envpol.2020.114098>
- Li Q, Chen Z, Wang H, Yang H, Wen T, Wang S, Hu B, Wang X (2021) Removal of organic compounds by nanoscale zero-valent iron and its composites. *Sci Total Environ* 792:148546. <https://doi.org/10.1016/j.scitotenv.2021.148546>
- Li S, Tang J, Yu C, Liu Q, Wang L (2022) Efficient degradation of anthracene in soil by carbon-coated nZVI activated persulfate. *J Hazard Mater* 431:128581. <https://doi.org/10.1016/j.jhazmat.2022.128581>
- Li F, Wang X, Xu C (2023) Research progress on structural characteristics, structure-application relationships, and environmental application of biochar-supported zero valent iron (ZVI-BC). *Curr Pollution Rep*. <https://doi.org/10.1007/s40726-023-00260-z>
- Liu CM, Diao ZH, Huo WY, Kong LJ, Du JJ (2018) Simultaneous removal of Cu²⁺ and bisphenol A by a novel biochar-supported zero valent iron from aqueous solution: synthesis, reactivity and mechanism. *Environ Pollut* 239:698–705. <https://doi.org/10.1016/j.envpol.2018.04.084>
- Liu Q, Sheng Y, Wang W, Liu X (2021) Efficacy and microbial responses of biochar-nanoscale zero-valent during in-situ remediation of Cd-contaminated sediment. *J Clean Prod* 287:125076. <https://doi.org/10.1016/j.jclepro.2020.125076>
- Machado S, Pinto SL, Grosso JP, Nouws HPA, Albergaria JT, Delerue-Matos C (2013) Green production of zero-valent iron nanoparticles using tree leaf extracts. *Sci Total Environ* 445–446:1–8. <https://doi.org/10.1016/j.scitotenv.2012.12.033>
- Maletić S, Kragulj Isakovski M, Sigmund G, Hofmann T, Hüffer T, Beljin J, Rončević S (2022) Comparing biochar and hydrochar for reducing the risk of organic contaminants in polluted river sediments used for growing energy crops. *Sci Total Environ* 843:157122. <https://doi.org/10.1016/j.scitotenv.2022.157122>
- Mirzaee E, Sartaj M (2023) Remediation of PAH-contaminated soil using a combined process of soil washing and adsorption by nano iron oxide/granular activated carbon composite. *Environ Nanotechnol Monit Manag* 20:100800. <https://doi.org/10.1016/j.enmm.2023.100800>
- Official Gazzete (2010) Ministry of Energy, Development and the Environment, Regulation on categories, testing and classification of waste. *The Official Gazette* 56/2010
- Official Gazette (2012) Regulation on limit values for pollutants in surface and groundwaters and sediments, and the deadlines for their achievement. *Belgrade, Serbia. Gazette No. 50/2012*
- Oleszczuk P, Kołtowski M (2017) Effect of co-application of nano-zero valent iron and biochar on the total and freely dissolved polycyclic aromatic hydrocarbons removal and toxicity of contaminated soils. *Chemosphere* 168:1467–1476. <https://doi.org/10.1016/j.chemosphere.2016.11.100>
- Patel HA, Bajaj HC, Jasra RV (2008) Synthesis of Pd and Rh metal nanoparticles in the interlayer space of organically modified montmorillonite. *J Nanopart Res* 10:625–632. <https://doi.org/10.1007/s11051-007-9292-9>. Accepted 7 Aug 2007
- Poguberović S, Krčmar D, Maletić S, Konya Z, Tomašević Pilipović D, Kerkez Đ, Rončević S (2016) Removal of As(III) and Cr(VI) from aqueous solutions using “green” zero-valent iron nanoparticles produced by oak, mulberry and cherry leaf extracts. *Ecol Eng* 90:42–49. <https://doi.org/10.1016/j.ecoleng.2016.01.083>
- Posada-Baquero R, Martín ML, Ortega-Calvo JJ (2019) Implementing standardized desorption extraction into bioavailability-oriented bioremediation of PAH-polluted soils. *Sci Total Environ* 696:134011. <https://doi.org/10.1016/j.scitotenv.2019.134011>
- Qiao J-t, Liu T-x, Wang X-q, Li F-b, Lv Y-h, Cui J-h, Zeng X-d, Yuan Y-z, Liu C-p (2018) Simultaneous alleviation of cadmium and arsenic accumulation in rice by applying zero-valent iron and biochar to contaminated paddy soils. *Chemosphere* 195:260–271. <https://doi.org/10.1016/j.chemosphere.2017.12.081>
- Quevauviller P, Rauret G, Rubio R, Lopez-Sanchez JF, Ure A, Bacon J, Muntau H (1997) Certified reference materials for the quality control of EDTA- and acetic acid-extractable contents of trace elements in sewage sludge amended soils (CRMs 483 and 484). *Fresenius J Anal Chem* 357:611–618. <https://doi.org/10.1007/s002160050222>
- Rani M, Shanker U (2018) Remediation of polycyclic aromatic hydrocarbons using nanomaterials. In: Crini, G., Lichtfouse, E. (eds) *Green Adsorbents for Pollutant Removal*. Springer Cham
- Roncevic S, Spasojevic J, Maletic S, Molnar Jazic J, Kragulj Isakovski M, Agbaba J, Grgic M, Dalmacija B (2016) Assessment of the bioavailability and phytotoxicity of sediment spiked with polycyclic aromatic hydrocarbons. *Environ Sci Pollut Res* 23(4):3239–3246. <https://doi.org/10.1007/s11356-015-5566-4>
- Ruiz-Torres C, Araujo-Martínez RF, Martínez-Castañón GA, Morales-Sánchez JE, Guajardo-Pacheco JM, González-Hernández J, Lee T-J, Shin H-S, Hwang Y, Ruiz F (2018) Preparation of air stable nanoscale zero valent iron functionalized by ethylene glycol without inert condition. *J Chem Eng* 336:112–122. <https://doi.org/10.1016/j.cej.2017.11.047>
- Shahid M, Austruy A, Echevarria G, Arshad M, Sanaullah M, Aslam M, Nadeem M, Nasim W, Dumat C (2014) EDTA-enhanced phytoremediation of heavy metals: a review. *Soil Sediment Contam* 23(4):389–416. <https://doi.org/10.1080/15320383.2014.831029>
- Shi L, Lin Y, Zhang X, Chen Z (2011) Synthesis, characterization and kinetics of bentonite supported nZVI for the removal of Cr(VI) from aqueous solution. *J Chem Eng* 171:612–617. <https://doi.org/10.1016/j.cej.2011.04.038>
- Siligardi C, Miselli P, Francia E, Lassinantti Gualtieri M (2017) Temperature-induced microstructural changes of fiber-reinforced silica aerogel (FRAB) and rock wool thermal insulation materials: a comparative study. *Energy Build* 138:80–87. <https://doi.org/10.1016/j.enbuild.2016.12.022>
- Sivodia C, Sinha A (2022) Clay supported zero valent iron nanocomposites: advancement in the field of green catalyst for abatement of persistent pollutant. In: Singh, S.P., Agarwal, A.K., Gupta, T., Maliyekkal, S.M. (eds) *New Trends in Emerging Environmental Contaminants*. Springer Singapore
- Slijepčević N, Tomašević Pilipović D, Kerkez Đ, Krčmar D, Bečelić-Tomin M, Beljin J, Dalmacija B (2021) A cost effective method for immobilization of Cu and Ni polluted river sediment with nZVI synthesized from leaf extract. *Chemosphere* 263:127816. <https://doi.org/10.1016/j.chemosphere.2020.127816>
- Slijepčević N, Kerkez Đ, Tomašević Pilipović D, Bečelić-Tomin M, Krčmar D (2018) Use of two different approaches to the synthesis of nano zero valent iron for sediment remediation. *Glob NEST J* 21(4):455–460. <https://doi.org/10.30955/gnj.002649>
- Solimanzadeh A, Fekri M (2017) The application of green tea extract to prepare bentonite-supported nanoscale zero-valent iron and its performance on removal of Cr(VI): Effect of relative parameters and soil experiments. *Microporous Mesoporous Mater* 239:60–69. <https://doi.org/10.1016/j.micromeso.2016.09.050>
- Spasojevic JM, Maletic SP, Roncevic SD, Radnovic DV, Cucak DI, Trickovic JS, Dalmacija BD (2015) Using chemical desorption

- of PAHs from sediment to model biodegradation during bioavailability assessment. *J Hazard Mater* 283:60–69. <https://doi.org/10.1016/j.jhazmat.2014.09.013>
- Spasojević J, Maletić S, Rončević S, Grgić M, Krčmar D, Varga N, Dalmacija B (2018) The role of organic matter and clay content in sediments for bioavailability of pyrene. *Water Sci Technol* 77(1–2):439–447. <https://doi.org/10.2166/wst.2017.551>
- SRPS EN 12879:2007 (2007) Determination of organic matter content in soil as loss-on-ignition. (European Committee for standardization), United Kingdom
- SRPS ISO 10390:2007 (2007) Determination of pH value in soil. International standard, Geneva, Switzerland
- SRPS ISO 5667–12:2019 (2019) Water quality - sampling - part 12: guidance on sampling of sediment from riverbeds, lakes and estuaries. International standard, Geneva, Switzerland
- Staninska-Pieta J, Czarny J, Piotrowska-Cyplik A, Juzwa W, Wolko L, Nowak J, Cyplik P (2020) Heavy metals as a factor increasing the functional genetic potential of bacterial community for polycyclic aromatic hydrocarbon biodegradation. *Molecules* 25(2):319. <https://doi.org/10.3390/molecules25020319>
- Stefaniuk M, Oleszczuk P, Ok YS (2016) Review on nano zerovalent iron (nZVI): From synthesis to environmental applications. *J Chem Eng* 287:618–632. <https://doi.org/10.1016/j.cej.2015.11.046>
- Su H, Fang Z, Tsang PE, Fang J, Zhao D (2016) Stabilisation of nanoscale zero-valent iron with biochar for enhanced transport and in-situ remediation of hexavalent chromium in soil. *Environ Pollut* 214:94–100. <https://doi.org/10.1016/j.envpol.2016.03.072>
- Sutherland RA (2002) Comparison between non-residual Al, Co, Cu, Fe, Mn, Ni, Pb and Zn released by a three-step sequential extraction procedure and a dilute hydrochloric acid leach for soil and road deposited sediment. *Appl Geochemistry* 17:353–365. [https://doi.org/10.1016/S0883-2927\(01\)00095-6](https://doi.org/10.1016/S0883-2927(01)00095-6)
- Tomašević Pilipović D, Kerkez Đ, Dalmacija B, Slijepčević N, Krčmar D, Rađenović D, Bečelić-Tomin M (2018) Remediation of toxic metal contaminated using three types of nZVI supported materials. *Bull Environ Contam Toxicol* 101:725–731. <https://doi.org/10.1007/s00128-018-2442-1>
- USEPA (Environmental Protection Agency) (2002) Method 1311: toxicity characteristic leaching procedure. www.epa.gov/SW-846/1311.pdf. Washington, D.C. United States
- USEPA (Environmental Protection Agency) (1995) Method 3550B: ultrasonic extraction. D.C., United States, Washington
- USEPA (Environmental Protection Agency) (1996a) Method 3630C: silica gel cleanup. D.C. United States, Washington
- USEPA (Environmental Protection Agency) (1996b) Method 8270D: semivolatile organic compounds by gas chromatography/mass spectrometry (GC/MS). D.C. United States, Washington
- USEPA (Environmental Protection Agency) (2007a) Method 3051a: microwave assisted acid digestion of sediments, sludges, soils and Revision 1. D.C. United States, Washington
- USEPA (Environmental Protection Agency) (2007b) Method 7000B: flame atomic absorption spectrophotometry, Revision 2. D.C. United States, Washington
- USEPA (Environmental Protection Agency) (2007c) Method 7010: graphite furnace absorption spectrophotometry, Revision 0. D.C. United States, Washington
- Wang Q, Qian H, Yang Y, Zhang Z, Naman C, Xu X (2010) Reduction of hexavalent chromium by carboxymethyl cellulose-stabilized zero-valent iron nanoparticles. *J Contam Hydrol* 114:35–42. <https://doi.org/10.1016/j.jconhyd.2010.02.006>
- Wang H, Liu T, Feng S, Zhang W (2017) Metal removal and associated binding fraction transformation in contaminated river sediment washed by different types of agents. *PLoS ONE* 12:1–14. <https://doi.org/10.1371/journal.pone.0174571>
- Wang B, Jin Z, Xu X, Zhou H, Yao X, Ji F (2019a) Effect of Tenax addition amount and desorption time on desorption behaviour for bioavailability prediction of polycyclic aromatic hydrocarbons. *Sci Total Environ* 651:427–434. <https://doi.org/10.1016/j.scitotenv.2018.09.097>
- Wang S, Zhao M, Zhou M, Li YC, Wang J, Gao B, Shinjiro S, Feng K, Yin W, Igalavithana AD, Oleszczuk P, Wang X, Ok YS (2019b) Biochar-supported nZVI (nZVI/BC) for contaminant removal from soil and water: a critical review. *J Hazard Mater* 373:820–834. <https://doi.org/10.1016/j.jhazmat.2019.03.080>
- Yang F, Zhang S, Sun Y, Cheng K, Li J, Tsang DCW (2018) Fabrication and characterization of hydrophilic corn stalk biochar-supported nanoscale zero-valent iron composites for efficient metal removal. *Bioresour Technol* 265:490–497. <https://doi.org/10.1016/j.biortech.2018.06.029>
- Yang J, Wang S, Xu N, Ye Z, Yang H, Huangfu X (2021) Synthesis of montmorillonite-supported nano-zero-valent iron via green tea extract: enhanced transport and application for hexavalent chromium removal from water and soil. *J Hazard Mater* 419:126461. <https://doi.org/10.1016/j.jhazmat.2021.126461>
- Ye J, Luo Y, Sun J, Shi J (2021) Nanoscale zero-valent iron modified by bentonite with Enhanced Cr(VI) removal efficiency, improved mobility, and reduced toxicity. *Nanomaterials* 11:2580. <https://doi.org/10.3390/nano11102580>
- Žemberyová M, Barteková J, Závadská M, Šišoláková M (2007) Determination of bioavailable fractions of Zn, Cu, Ni, Pb and Cd in soils and sludges by atomic absorption spectrometry. *Talanta* 71(4):1661–1668. <https://doi.org/10.1016/j.talanta.2006.07.055>
- Zhang M, Gao B (2013) Removal of arsenic, methylene blue, and phosphate by biochar/AlOOH nanocomposite. *J Chem Eng* 226:286–292. <https://doi.org/10.1016/j.cej.2013.04.077>
- Zhang M, Li J, Wang Y (2019) Impact of biochar-supported zerovalent iron nanocomposite on the anaerobic digestion of sewage sludge. *Environ Sci Pollut Res* 26:10292–10305. <https://doi.org/10.1007/s11356-019-04479-6>
- Zhang Y, Jiao X, Liu N, Lv J, Yang Y (2020) Enhanced removal of aqueous Cr(VI) by green synthesized nanoscale zero-valent iron supported on oak wood biochar. *Chemosphere* 245:125542. <https://doi.org/10.1016/j.chemosphere.2019.125542>
- Zhang Y, Labianca C, Chen L, De Gisi S, Notarnicola M, Guo B, Sun J, Ding S, Wang L (2021) Sustainable ex-situ remediation of contaminated sediment: a review. *Environ Pollut* 287:117333. <https://doi.org/10.1016/j.envpol.2021.117333>
- Zhao X, Liu W, Cai Z, Han B, Qian T, Zhao D (2016) An overview of preparation and applications of stabilized zerovalent iron nanoparticles for soil and groundwater remediation. *Water Res* 100:245–266. <https://doi.org/10.1016/j.watres.2016.05.019>
- Zimmerman AR, Gao B, Ahn MY (2011) Positive and negative carbon mineralization priming effects among a variety of biochar-amended soils. *Soil Biol Biochem* 43:1169–1179. <https://doi.org/10.1016/j.soilbio.2011.02.005>

Publisher's Note Springer Nature remains neutral with regard to jurisdictional claims in published maps and institutional affiliations.

Springer Nature or its licensor (e.g. a society or other partner) holds exclusive rights to this article under a publishing agreement with the author(s) or other rightsholder(s); author self-archiving of the accepted manuscript version of this article is solely governed by the terms of such publishing agreement and applicable law.